

Local buckling failure analysis of high-strength pipelines

Yan Li¹ · Jian Shuai¹ · Zhong-Li Jin² · Ya-Tong Zhao¹ · Kui Xu¹

Handling editor: Jin-Jiang Wang

Received: 12 December 2016 / Published online: 14 July 2017
© The Author(s) 2017. This article is an open access publication

Abstract Pipelines in geological disaster regions typically suffer the risk of local buckling failure because of slender structure and complex load. This paper is meant to reveal the local buckling behavior of buried pipelines with a large diameter and high strength, which are under different conditions, including pure bending and bending combined with internal pressure. Finite element analysis was built according to previous data to study local buckling behavior of pressurized and unpressurized pipes under bending conditions and their differences in local buckling failure modes. In parametric analysis, a series of parameters, including pipe geometrical dimension, pipe material properties and internal pressure, were selected to study their influences on the critical bending moment, critical compressive stress and critical compressive strain of pipes. Especially the hardening exponent of pipe material was introduced to the parameter analysis by using the Ramberg–Osgood constitutive model. Results showed that geometrical dimensions, material and internal pressure can exert similar effects on the critical bending moment and critical compressive stress, which have different, even reverse effects on the critical compressive strain. Based on these analyses, more accurate design models of critical bending moment and critical compressive stress have been proposed for high-strength pipelines under bending

conditions, which provide theoretical methods for high-strength pipeline engineering.

Keywords Local buckling · High-strength pipeline · Finite element analysis · Critical bending moment · Critical compressive stress · Critical compressive strain

1 Introduction

Local buckling is an ultimate state of pipelines under complex loading conditions caused by subsidence, earthquake and landslides, etc., in geological hazard zones (Han et al. 2012; Shantanu et al. 2011). Local gross deformation in wrinkled sections can do harm to loading-carrying capacity and even damage structure integrity of pipelines (Dama et al. 2007). Technological advances have resulted in high-strength pipe steel being widely used for long-distance transmission of natural gas. However, an increase in the diameter/thickness ratio of high-strength pipe steel makes pipelines more and more susceptible to local buckling failure. Several researchers have begun to study the difference of material properties between high-strength pipe steel and traditional pipe steel (Chen et al. 2008; Igi et al. 2008; Timms et al. 2009; Suzuki et al. 2010). Traditional high-strength pipelines typically have higher yield ratio and lower strain capacity compared with medium-strength pipelines (Fathi et al. 2010). However, the high strain pipelines exhibit excellent strain capacity, which is equal or better than traditional strength pipelines, and favorable to structural behavior (Nobuhisa et al. 2008). Based on the study of high-strength pipelines crossing strike-slip faults, Liu et al. (2016) suggested that the high-strength steel has a significant influence on the critical

✉ Jian Shuai
sjclass@126.com

¹ Faculty of Mechanical and Transportation Engineering, China University of Petroleum, Beijing 102249, China

² China ENFI Engineering Corporation, Beijing 100038, China

stress along the axial direction. Therefore, more comprehensive research on local buckling mechanisms in high-strength pipelines is of great importance to prevent local buckling failure from occurring.

Critical buckling theory was introduced in the 1960s, and experiments and numerical simulations have later been conducted to investigate the local buckling of pressurized pipes (Dorey and Cheng 2001; Dorey et al. 2002, 2005). Also, several prediction methods were established to evaluate the ultimate state (Paquette and Kyriakides 2006; Limam et al. 2010) and are mostly used to calculate the critical bending moment and the critical compressive strain. Mohareb (1995) investigated the local buckling behavior through examining several plain pipes and proposed the ‘Mohareb–Murray interaction equation’ to determine the critical bending moment based on an ideal elastoplastic material model. ABS standard (ABS 2006) put forward a model to determine the maximum allowable moment. However, both methods have some weaknesses. Specifically, the model in the ABS standard is only applicable for pipes with a diameter/thickness ratio of 10–60, which cannot be used in pipes with larger diameter/thickness ratio. Also, it is limited by practicable materials and ignoring strain hardening effect; the ‘Mohareb–Murray interaction equation’ and model in ABS may overestimate or underestimate the critical bending moment (Nazemi 2009). Thus, accurately determining the critical bending moment is a crucial issue for predicting local buckling behavior. Currently, the critical compressive strain has been studied for a long time and some results have been used in practical standards, e.g., the formulation from Murphey and Langner (Gresnigt and Foeken 2001) has been used in American Bureau of Shipping (ABS 2006) and the research conducted by Gresnigt (1986) has been adopted by Canadian Standards Association (CSA 2007). Also, other standards provide similar design formulae of critical compressive strain (ASCE 1984; ALA 2001), which have been widely used in engineering design. However, critical compressive stress is currently poorly understood. Plantema studied the buckling stress of circular cylinders and round tubes under compression conditions (Ahn et al. 2016), which are not applicable under bending loading conditions. These models mentioned above have not comprehensively considered the critical properties of strain hardening of high-strength pipelines with bending load. Thus, in this paper, the primary concern is about the local buckling of high-strength pipelines.

In this paper, a practical three-dimensional model was established using the nonlinear finite element method (FEM) and calibrated with previous experimental results (Zimmerman et al. 2004). After that, deformation behavior and different failure modes of unpressurized and pressurized pipes were studied under bending conditions. The

influences of pipe diameter, pipe wall thickness, yield strength, hardening exponent and internal pressure on deformation behavior of local buckling of high-strength pipelines were analyzed in detail. Finally, methods were proposed to predict the critical bending moment and critical compressive stress of local buckling of high-strength pipelines under bending load and demonstrated with an application example.

2 Numerical simulation

Laboratory testing is an effective way to obtain first-hand data, but it is costly and time-consuming. Alternatively, numerical simulations can provide a fast, convenient and cost-efficient way to study local buckling. The bearing capacity of submarine and long-distance transmission pipelines are mainly depending on pipe dimensions, material properties and loading conditions (Dang et al. 2010; Sun 2013), which can be determined by detailed parametric analysis. So the first thing is to establish a proper finite element model to do the parametric analysis.

2.1 Finite element model

Commercial nonlinear finite element software, ABAQUS, was used to develop the three-dimensional nonlinear finite element model. Although the wrinkled section of local buckling distributes within a limited area, the pipe length is important for investigating deformation behavior of local buckling. To avoid end effects, the pipe length is supposed to be 3.5 times larger than the pipeline diameter (Ozkan and Mohareb 2009b). Therefore, a pipe with a length of $L = 6D$ was used in this study. Models were constructed using solid elements, which have been proved a reliable tool for simulating local buckling of pipes (Ozkan and Mohareb 2009a). Finally, a modified RIKS algorithm in ABAQUS has been used to perform finite element simulations.

2.2 Loading and boundary conditions

A fixed constraint is applied to one end of the pipe, and a bending moment is applied to the other end by a coupling constraint. Pressure is applied on the internal surface. Under pure bending conditions, the bending moment is the only load, which increases monotonically until local buckling occurs. Under mixed loading conditions, the finite element analysis is conducted with two steps: pressure loading step and bending step. Pressure is set as a constant internal pressure, while bending is the same as that under pure bending conditions. The finite element model is shown in Fig. 1, with element type of C3D20R and the element size of 4.7 mm × 35 mm × 35 mm.

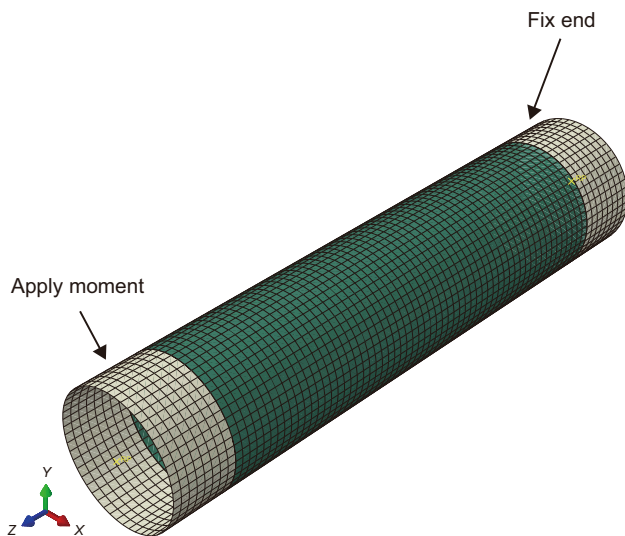


Fig. 1 Finite element model

2.3 Material parameters

With increasing demand for natural gas, high-strength steel pipelines have been widely used for long-distance transmission of natural gas in China. Two typical high-strength pipeline steels X70 and X80 are established in the FEM simulations. The nonlinearity of materials can be described by the Ramberg–Osgood constitutive model (Ramberg and Osgood 1943; Kamaya 2016). The constitutive relationship can be expressed as follows:

$$\varepsilon = \frac{\sigma}{E} + \alpha \left(\frac{\sigma}{\sigma_s} \right)^n \quad (1)$$

where ε is the true strain; σ is the true stress; E is the elastic modulus; σ_s is the yield strength that is defined at 0.5% strain; n is the hardening exponent; α is the “yield” offset.

2.4 Model calibration

In order to evaluate the validity of the numerical simulation, the results were calibrated with previous experimental results (Zimmerman et al. 2004). Four specimens were used to study the local buckling behavior in experiments, including two material grades X70 and X80. Figure 2 and Table 1 show the corresponding stress–strain curves and material parameters, respectively. One specimen of each material was tested under pure bending conditions, and the other was tested under bending conditions with a maximum operation pressure of 80% specified minimum yield strength (SMYS). Detailed test data are listed in Table 2.

Selecting a reasonable length is crucial for numerical simulation, because the value of the critical compressive strain varies with the effective length of the pipe. Previous studies demonstrate that buckles typically occur within the

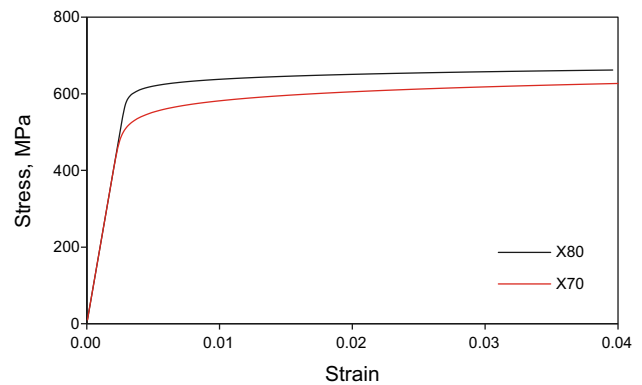


Fig. 2 Stress–strain curves of X70 and X80

length of $1D$ in the axial direction (Mohareb 1995; Ozkan and Mohareb 2009b). With this assumption, the relationship between moment and compressive strain was plotted in Fig. 3, which can be used to calculate the critical bending moments. The results of three methods are listed in Table 3. The critical bending moments obtained from FEM are generally correctly predicted with an error within 4.23%, which is better than the Mohareb and the ABS method.

Figure 3 suggests that the buckling trend obtained by FEM agrees well with experimental results. At first, the compressive strain increases with bending moment. When the bending moment reaches the maximum value, local buckling occurs, and then the bending moment begins to decrease, the strain still increases until the pipe loses its loading capacity completely. The maximum value of bending moment is the critical bending moment, and corresponding compressive strain is the critical compressive strain. The buckling mode exhibits two main failure shapes, which can be observed in both experimental results and FEM results (Fig. 4a–d). The unpressurized pipe buckled in a “diamond shape,” while the pressurized pipe buckled in a pipe wall outward bulging shape.

3 Parametric analysis

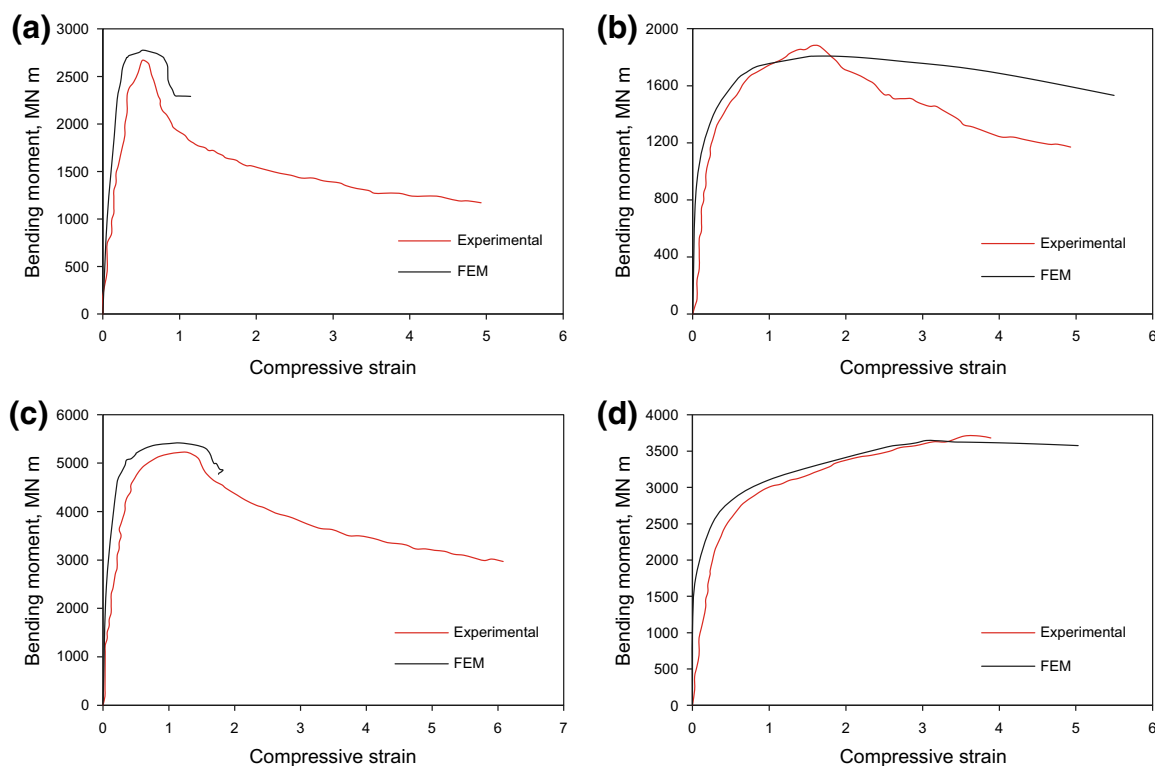
An excessive load induced by pressure and bending leads to local buckling of a pipeline, while the failure behavior of local buckling can be described by the critical bending moment, critical compressive stress and the critical compressive strain. The critical bending moment is defined as the maximum moment at the critical point of bending vs. compressive strain curve, while the corresponding stress and strain are critical compressive stress and critical compressive strain. These three parameters primarily vary as a function of several variables, which can be divided into three types: geometrical parameters, material

Table 1 Material parameters of X70 and X80

Material grade	Elastic modulus E , MPa	Poisson's ratio ν	Yield strength σ_s , MPa	Yield offset α	Hardening exponent n
X70	200,000	0.3	552	0.81	22
X80	200,000	0.3	620	0.61	45

Table 2 Test data and loading conditions

Specimen No.	Material grade	Pipe outer diameter D , mm	Pipe wall thickness t , mm	D/t	Pressure
U70	X70	762	9.4	82	0
P70	X70	762	9.4	82	80% SMYS
U80	X80	762	15.7	48	0
P80	X80	762	15.7	48	80% SMYS

**Fig. 3** Bending moment versus compressive strain curves of four specimens. **a** U70: X70 unpressurized pipe. **b** P70: X70 pressurized pipe. **c** U80: X80 unpressurized pipe. **d** P80: X80 pressurized pipe

parameters and load parameter. It is essential to analyze the influence of these parameters on local buckling behavior under bending when designing long-distance pipelines. In the analysis, only one parameter is changed at a time and others are taken as the basic values. Specifically, the basic values of geometrical parameters include the diameter and wall thickness of pipes, which were selected based on real pipeline dimensions and design code for gas pipeline

engineering. The geometrical dimensions (diameter and wall thickness) of pipes used for X701 (X801), X702 (X802) and X703 (X803) are 813 mm \times 11.7 mm, 1016 mm \times 14.6 mm, 1219 mm \times 15.3 mm, respectively. The basic values of material parameters include yield strength and hardening exponent. Specifically, the yield strengths of basic pipe materials (pipe grade X70 and X80) are 580 and 641 MPa, while the hardening exponents

Table 3 Comparison of critical bending moment obtained from test and other different methods

Specimen No.	Experimental value, MN m	FEM		Mohareb		ABS	
		Value, MN m	Error, %	Value, MN m	Error, %	Value, MN m	Error, %
U70	2667	2776	4.09	2939	10.20	2042	−23.43
P70	1845	1808	−2.01	2412	30.73	1176	−36.26
U80	5198	5417	4.22	5421	4.29	4032	−22.43
P80	3718	3646	−4.23	4408	18.56	2092	−43.73

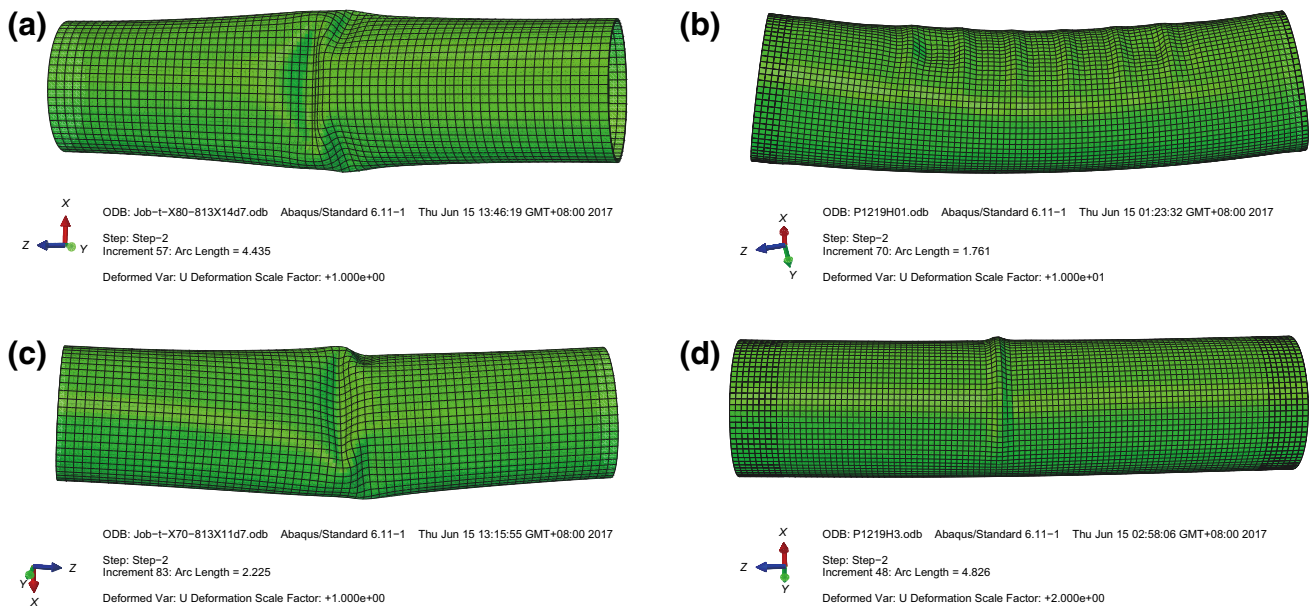


Fig. 4 Buckling shape obtained from FEM. **a** U70: X70 unpressurized pipe. **b** P70: X70 pressurized pipe. **c** U80: X80 unpressurized pipe. **d** P80: X80 pressurized pipe

are 10.0 and 17.15, respectively. The load parameter is the internal pressure that varies with the maximum operating pressure (MAOP). Detailed parameter descriptions are included in Table 4.

3.1 Critical bending moment

As a key parameter of local buckling, the critical bending moment is correlated with the pipe dimensions, pipe material properties and the internal pressure. In terms of pipe dimensions, both the pipe diameter and thickness can enhance the pipe stiffness. Figure 5 shows that the critical bending moment increases exponentially with the pipe diameter. And for a certain diameter, the higher the pipe grade, the higher the critical bending moment. Figure 6 shows that the critical bending moment increases linearly with thickness.

To analyze the effect of pipe material properties on the critical bending moment, the initial value was taken as the SMYS specified in the standard. The critical bending moment vs. yield strength (Fig. 7) exhibits that the critical bending moment increases linearly with the yield strength. With the same yield strength, the critical bending moment of X802 is lower than that of X702. It is because the hardening exponent of X80 pipes is larger than that of X70 pipes. Figure 8 shows that the critical bending moment decreases nonlinearly with hardening exponent. With the same hardening exponent, the critical bending moment of higher grade pipes is larger.

For pressurized pipes, as Fig. 9 shows, the critical bending moment decreases exponentially with the internal pressure. Compared with X70 grade pipes, the critical bending moment of X80 grade pipes decreases more rapidly.

Table 4 Ranges of parameters used in FEM

Parameter type	Basic values	Range of univariate analysis
Diameter D , mm	X701, X801: 813 X702, X802: 1016 X703, X803: 1219	813–1219
Thickness t , mm	X701, X801: 11.7 X702, X802: 14.6 X703, X803: 15.3	X701: 11.7–21 X801: 10.2–21 X702: 14.6–26.2 X802: 12.8.2–24 X703: 17.5–31.5 X803: 15.3–31.5
Yield strength σ_s , MPa	X70: 580 X80: 641	X70: 490–580 X80: 560–641
Hardening exponent n	X70: 10.0 X80: 17.5	5–25
Internal pressure P , MPa	0	0-MAOP

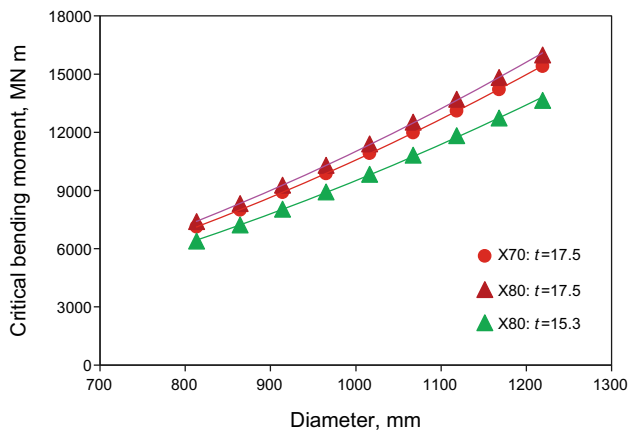


Fig. 5 Relationship between the critical bending moment and the pipe diameter

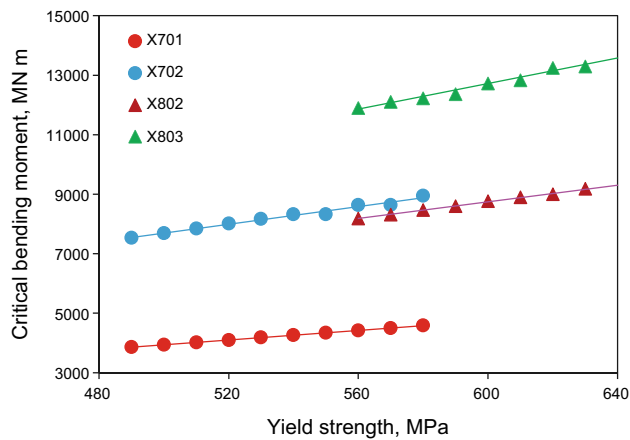


Fig. 7 Relationship between the critical bending moment and the yield strength

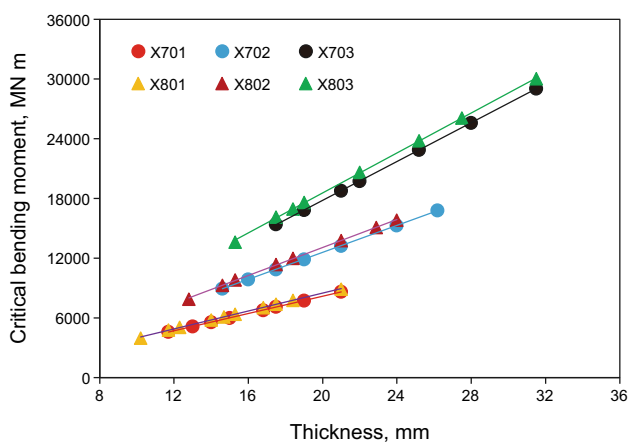


Fig. 6 Relationship between the critical bending moment and the wall thickness

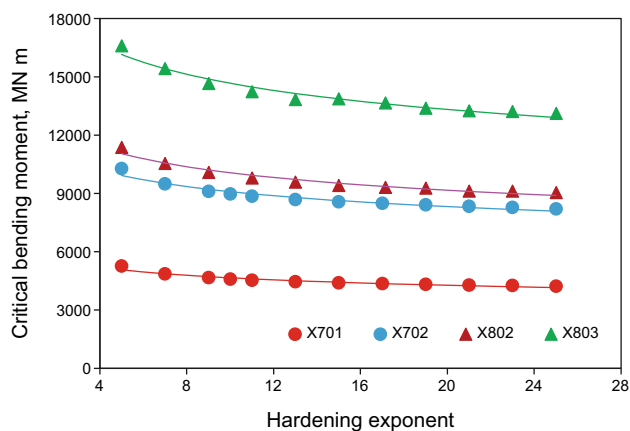


Fig. 8 Relationship between the critical bending moment and the hardening exponent

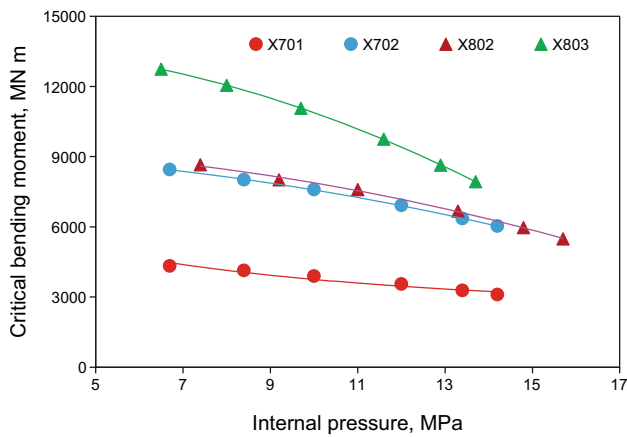


Fig. 9 Relationship between the critical bending moment and the internal pressure

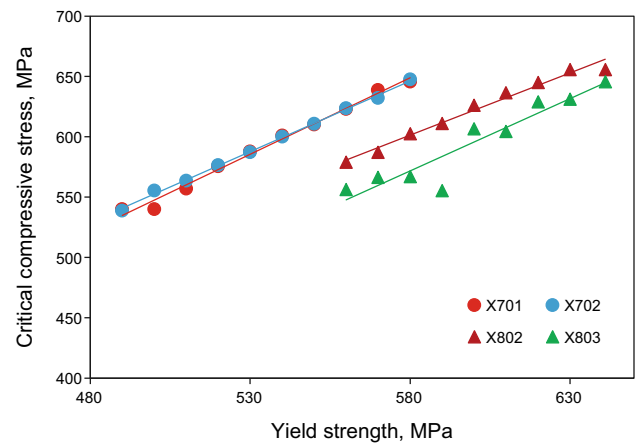


Fig. 11 Relationship between the critical compressive stress and the yield strength

3.2 Critical compressive stress

Stress and strain can be used to determine the structural behavior under loading conditions. In terms of the geometrical dimensions of pipes, the critical compressive stress increases with thickness and decreases with diameter. Thus, the effect of geometrical dimensions on the critical compressive stress can be illustrated by the thickness/diameter ratio. As Fig. 10 shows, the critical compressive stress increases near-linearly with the thickness/diameter ratio.

In terms of pipe material properties, two pipe grades, X70 and X80, were used in this study. Figure 11 shows that the critical compressive stress increases linearly with the yield strength. The hardening exponent of X80 grade pipe is higher than that of the X70 grade pipe; whereas the critical compressive stress of the former is lower than that of the latter. It should be noted that X701 and X702 almost

coincide, but there is some difference between X801 and X802. This can be explained by the fact that X701 and X702 have the same thickness/diameter ratio, which differs from that of X801 and X802. Figure 12 shows that the critical compressive stress decreases nonlinearly with the hardening exponent. With the same hardening exponent, the critical compressive stress of X80 grade pipe is larger than that of X70 grade pipes. This is because the yield strength of higher grade pipes is larger, so the stress state level of higher grade pipes is higher.

As Fig. 13 suggests, the internal pressure has a negative influence on the critical compressive stress, and at the same internal pressure, the critical compressive stress of the X80 grade pipe is lower than that of the X70 grade pipe. A comparison between X80 grade pipe and X70 grade pipe indicates that the critical compressive stress decreases rapidly as the pipe grade becomes higher.

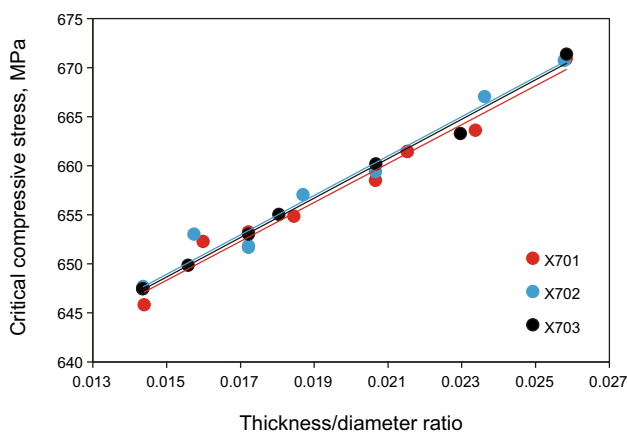


Fig. 10 Relationship between the critical compressive stress and the thickness/diameter ratio

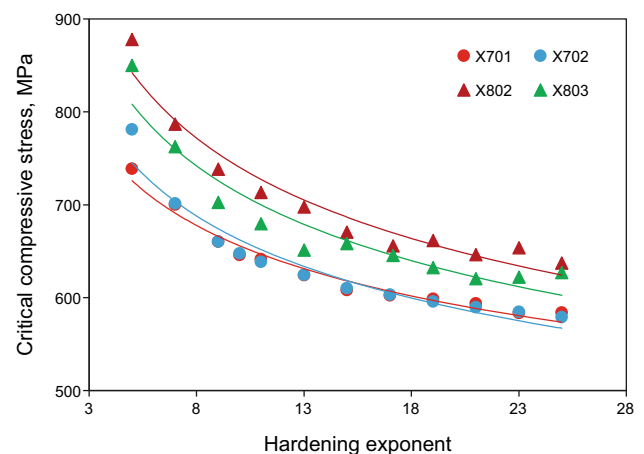


Fig. 12 Relationship between the critical compressive stress and the hardening exponent

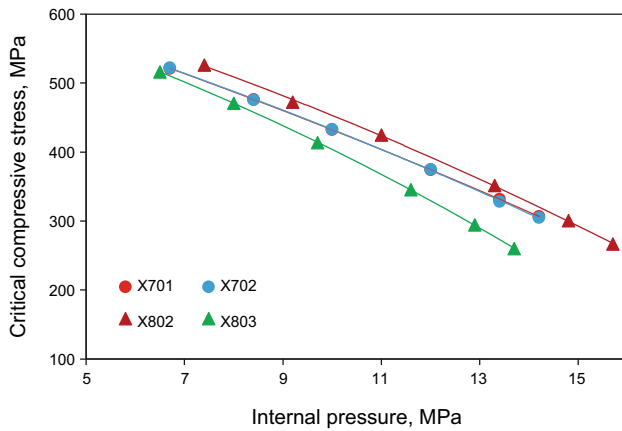


Fig. 13 Relationship between the critical compressive stress and the internal pressure

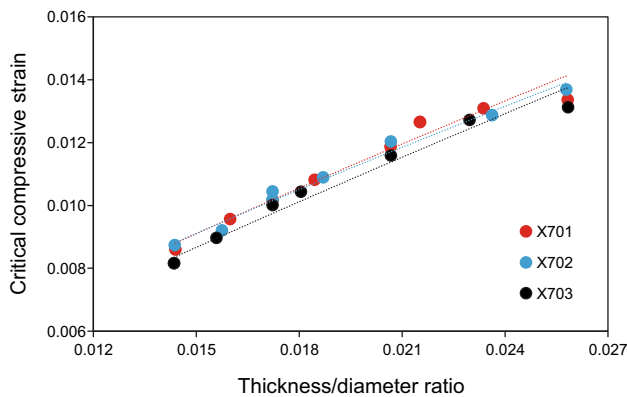


Fig. 14 Relationship between the critical compressive strain and the thickness/diameter ratio

3.3 Critical compressive strain

The critical compressive strain refers to the critical point where the structure loses its stability. It should be noted that the critical compressive strain is a strain design for local buckling, not for other failure modes. The critical compressive strain increases near-linearly with the thickness/diameter ratio, which is similar to the relationship between the critical compressive stress and the thickness/diameter ratio (Fig. 14). Figure 15 shows no significant variation of critical compressive strain with yield strength, indicating that the critical compressive strain is insensitive to the yield strength; also, the relationship between the critical compressive strain and the yield strength is significantly different from that between the critical compressive stress and the yield strength, which can be explained by the stress–strain state during the occurrence of local buckling. The local buckling typically occurs after yielding as Fig. 16 shows. The ratio of Mises

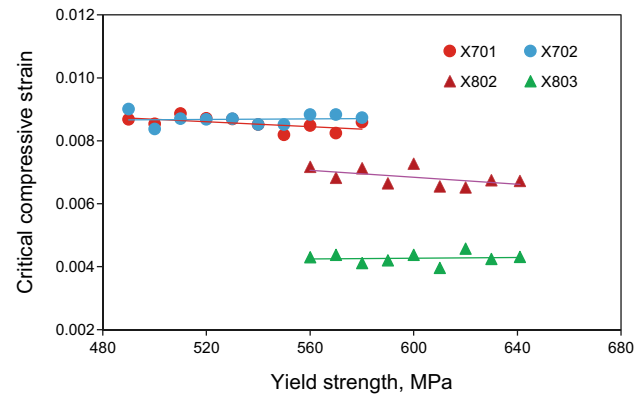


Fig. 15 Relationship between the critical compressive strain and the yield strength

stress to yield strength does not vary significantly among different materials.

The critical compressive strain decreases with an increase in the hardening exponent, which is similar to the critical compressive stress, while the critical compressive strains vary in a narrow range as Fig. 17 shows. The critical compressive strain increases nonlinearly with the internal pressure, and its value of the higher grade pipe (X802) is lower than that of the lower grade pipe (X702) (Fig. 18), which is different from the relationship between critical compressive stress and internal pressure.

4 Recommended design methods

4.1 Design methods

Over 300 finite element models with different parameters have been simulated by ABAQUS software, and the results are summarized in Sect. 3. It can be concluded that the critical bending moment of the locally buckled pipe has a highly positive correlation with the pipe diameter, pipe wall thickness, yield strength and the hardening exponent, and a negative correlation with the internal pressure. Importantly, the hardening exponent is considered as an important controlling factor of the critical bending moment. For the unpressurized pipe, the critical bending moment of local buckling can be calculated with Eq. (2), in which the hardening exponent is taken into consideration.

$$M = a_1 \cdot D^2 \cdot t \cdot \sigma_s \cdot n^{a_2} \quad (2)$$

where M is the critical bending moment of the unpressurized pipe, MN, m; D is the outer diameter of the pipe, mm; t is the wall thickness of the pipe, mm; σ_s is the yield strength of pipe material, MPa; n is the hardening exponent of the pipe material; a_1 and a_2 are the correlation coefficients.

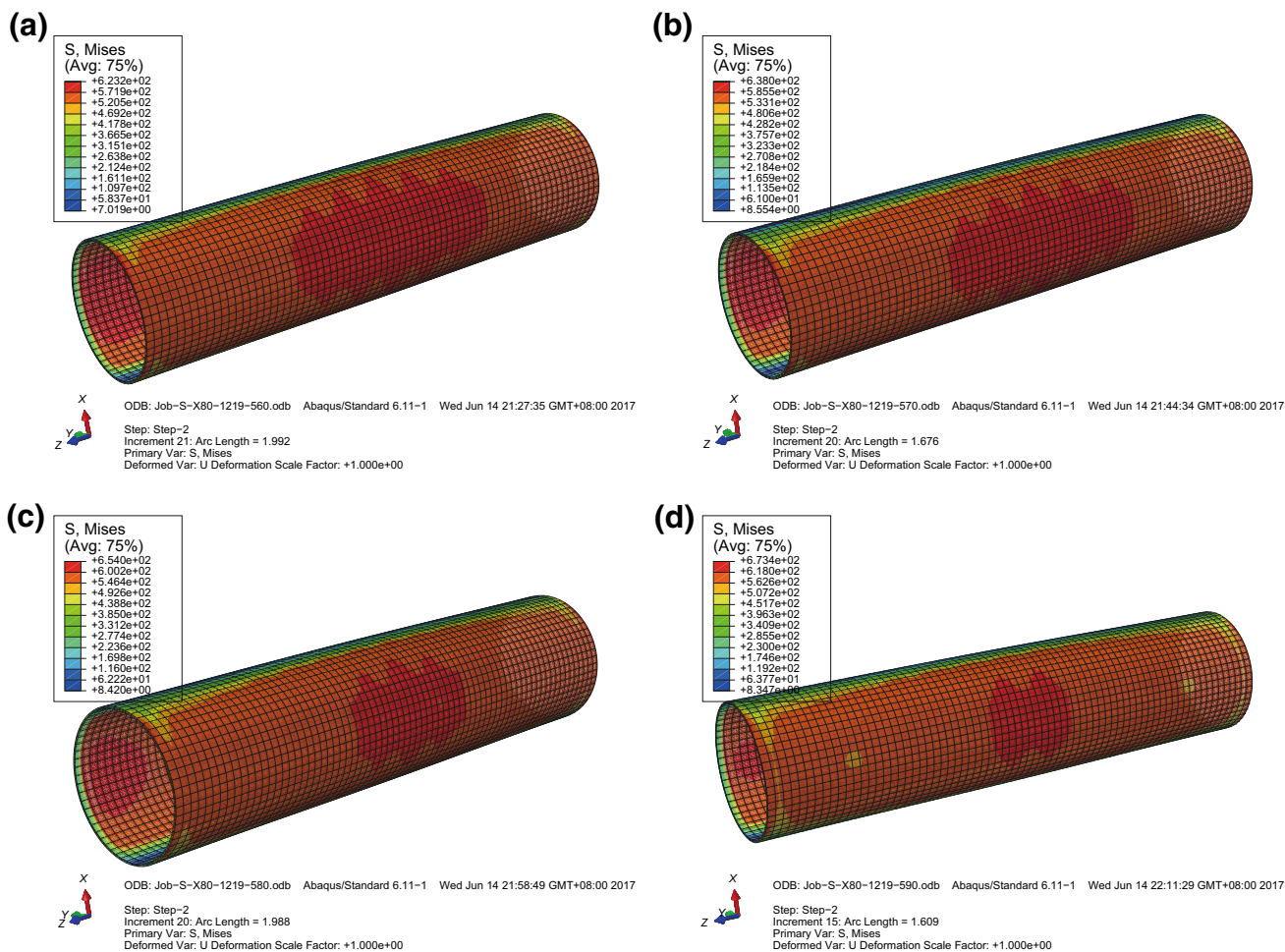


Fig. 16 Mises stress distribution at the local buckling state. **a** Yield strength $\sigma_s = 560$ MPa. **b** Yield strength $\sigma_s = 570$ MPa. **c** Yield strength $\sigma_s = 580$ MPa. **d** Yield strength $\sigma_s = 590$ MPa

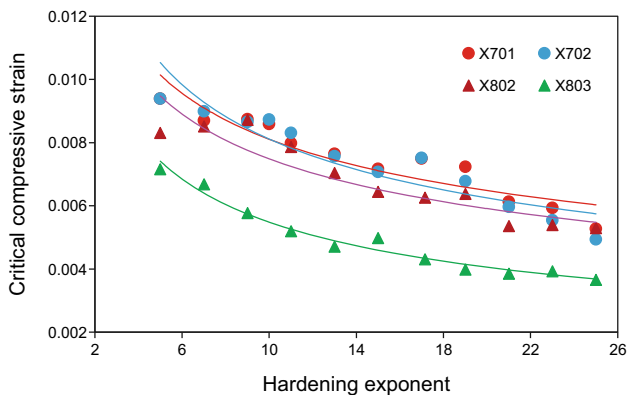


Fig. 17 Relationship between the critical compressive strain and the hardening exponent

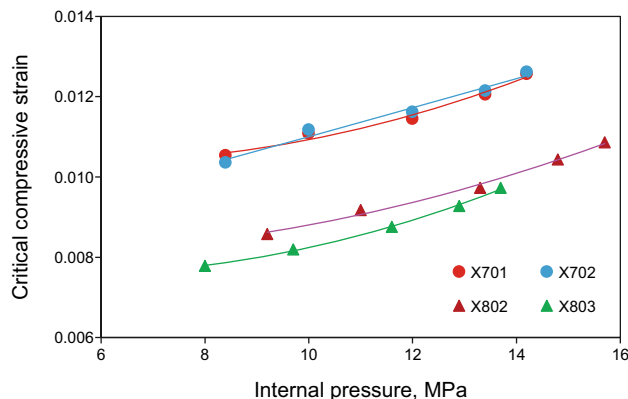


Fig. 18 Relationship between the critical compressive strain and the internal pressure

Based on Eq. (2), the critical bending moment of the pressurized pipe can be obtained by introducing the internal pressure as a quadratic polynomial, and described as follows:

$$M_p = M \cdot [b_1 \cdot (\sigma_\theta / \sigma_s)^2 + b_2] \tag{3}$$

where M_p is the critical bending moment of the pressurized pipe, MN m; σ_θ is the hoop stress of the pipe at the internal

pressure, MPa; b_1 and b_2 are the correlation coefficients. The related parameters can be obtained by fitting analysis, and the final calculation formulas are as follows:

$$M = 1.41 \cdot D^2 \cdot t \cdot \sigma_s \cdot n^{-0.13} \tag{4}$$

$$M_p = M \cdot \left[-0.576 \cdot (\sigma_\theta/\sigma_s)^2 + 0.99 \right] \tag{5}$$

Similarly, the critical compressive stress of local buckling positively correlates with the thickness/diameter ratio, yield strength and the hardening exponent, and negatively correlates with the internal pressure. Thus, the prediction model of unpressurized and pressurized pipes can be expressed as Eqs. (6) and (7). According to the fitting results, the final prediction model can be expressed as Eqs. (8) and (9).

$$\sigma_c = \sigma_s \cdot (c_1 \cdot t/D + c_2) \cdot (c_3^n + c_4) \tag{6}$$

$$\sigma_{cp} = \sigma_c \cdot [d_1 \cdot (\sigma_\theta/\sigma_s) + d_2] \tag{7}$$

$$\sigma_c = \sigma_s \cdot (4.66 \cdot t/D + 0.94) \cdot (0.8^n + 1) \tag{8}$$

$$\sigma_{cp} = \sigma_c \cdot [-0.77 \cdot (\sigma_\theta/\sigma_s) + 1.06] \tag{9}$$

where σ_c is the critical compressive stress of the unpressurized pipe, MPa; c_1 , c_2 and c_3 are the correlation coefficients; σ_{cp} is the critical compressive stress of the pressurized pipe, MPa; d_1 , d_2 and d_3 are the correlation coefficients.

4.2 Application of the proposed methods

X70 1016-mm and X80 1219-mm gas pipelines were used as application examples to demonstrate the proposed methods. Figures 19 and 20 show comparisons of the critical bending moment and the critical compressive stress obtained from different methods. The comparisons indicate

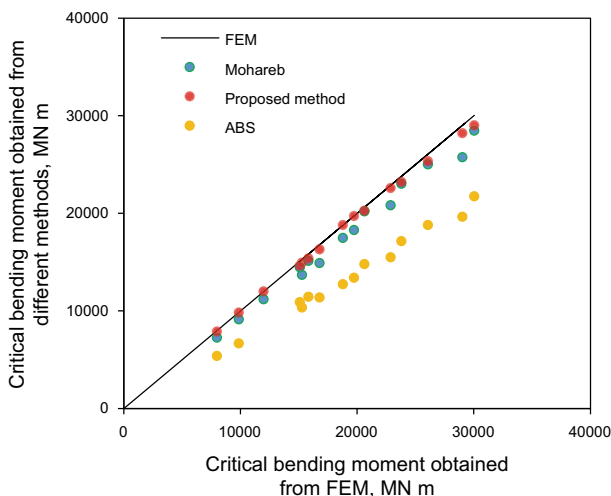


Fig. 19 Comparison of the critical bending moment obtained from different methods

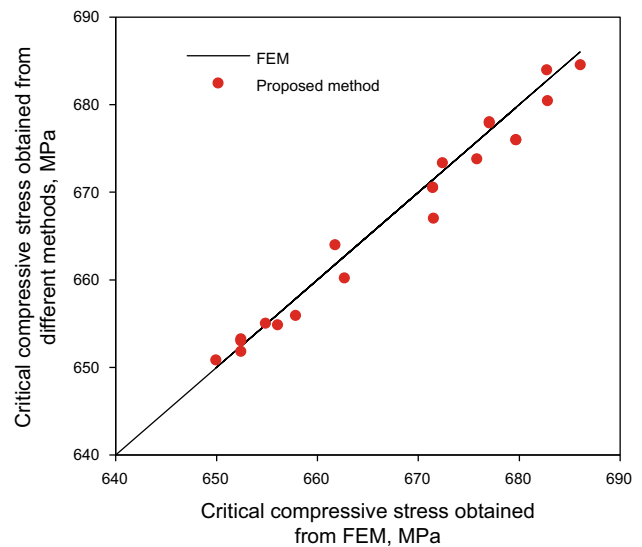


Fig. 20 Accuracy of the proposed method of critical compressive stress compared with FEM

that the proposed method can provide better estimates of both the critical bending moment and the critical compressive stress.

5 Conclusions

A finite element analysis model for local buckling was established based on the present work. The effects of key parameters including pipe diameter, pipe thickness, yield strength, hardening exponent and internal pressure, on the critical bending moment, critical compressive stress and the critical compressive strain have been investigated comprehensively through a series of models. Based on these parametric analysis results, the prediction models for critical bending moment and critical compressive stress were proposed and verified. The following conclusions can be drawn.

1. The critical bending moment of local buckling increases exponentially with the pipe diameter and increases linearly with the pipe thickness and the yield strength, while it decreases nonlinearly with an increase in the hardening exponent.
2. Local buckling occurs after the stress of the pipe reaches yield strength. Similar to the critical bending moment, the critical compressive stress increases linearly with the thickness/diameter ratio and the yield strength, and decreases exponentially with the hardening exponent and internal pressure.
3. The thickness/diameter ratio and hardening exponent have a similar influence on the critical compressive strain. However, the yield strength has no influence on

the critical compressive strain and has a linear relationship with the critical compressive stress.

- The parameter analysis demonstrates that local buckling behavior varies with hardening exponent. The calculation methods for the critical bending moment and the critical compressive stress were proposed based on the effect of the hardening exponent on local buckling behavior. These two methods were validated by comparing the results with FEM, and the comparison results showed high accuracy.

Acknowledgements The work is supported by the National Science-Technology Support Plan Projects of China, under Award No. 2015BAK16B02.

Open Access This article is distributed under the terms of the Creative Commons Attribution 4.0 International License (<http://creativecommons.org/licenses/by/4.0/>), which permits unrestricted use, distribution, and reproduction in any medium, provided you give appropriate credit to the original author(s) and the source, provide a link to the Creative Commons license, and indicate if changes were made.

References

- ABS. Guide for building and classing subsea pipeline systems. Houston: ABS; 2006.
- Ahn K, Lim IG, Yoon J, Huh H. A simplified prediction method for the local buckling load of cylindrical tubes. *Int J Precis Eng Manuf*. 2016;17(9):1149–56.
- ALA. Guidelines for the design of buried steel pipe. Chicago: ALA; 2001.
- ASCE. Guidelines for the seismic design of oil and gas pipeline systems. Reston: ASCE; 1984.
- Chen H, Ji L, Gong S, Gao H. Deformation behavior prediction of X80 steel line pipe and implication on high strain pipe specification. In: International pipeline conference. Calgary, Alberta, Canada. 2008.
- CSA. Oil and gas pipeline systems. CSA Z662-07, Ontario, Canada, 2007.
- Dama E, Karamanos SA, Gresnigt AM. Failure of locally buckled pipelines. *J Press Vessel Technol*. 2007;129(2):272–9. doi:10.1115/1.2716431.
- Dang XB, Gong SF, Jin WL, Li ZG, Zhao DY, Ning HE. Analysis on ultimate bearing capacity of deep-water submarine pipe. *J Zhejiang Univ (Eng Sci)*. 2010;44(4):778–82. doi:10.3785/j.issn.1008-973X.2010.04.027 (in Chinese).
- Dorey AB, Cheng JJR. Critical buckling strains in energy pipelines. Structural engineering report SER 237. Edmonton, 2001.
- Dorey AB, Murray DW, Cheng JJR. Material property effects on critical buckling strains in energy pipelines. In: International pipeline conference. 2002. pp. 475–84. doi:10.1115/IPC2002-27225.
- Dorey AB, Murray DW, Cheng JJR. Critical buckling strain equations for energy pipelines—a parametric study. *J Offshore Mech Arct Eng*. 2005;128(3):248–55. doi:10.1115/1.2199561.
- Fathi A, Cheng JJR, Adeeb S, Zhou J. Critical buckling strain in high strength steel pipes using isotropic-kinematic hardening. In: International pipeline conference. 2010. pp. 39–47.
- Gresnigt AM. Plastic design of buried steel pipelines in settlement areas. *Heron*. 1986;4(31).
- Gresnigt AM, Foeken RJV. Local buckling of UOE and seamless steel pipes. In: International offshore and polar engineering conference. Norway: The International Society of Offshore and Polar Engineers, 2001.
- Han B, Wang ZY, Zhao HL, Jing HY, Wu ZZ. Strain-based design for buried pipelines subjected to landslides. *Pet Sci*. 2012;9(2):236–41. doi:10.1007/s12182-012-0204-y.
- Igi S, Kondo J, Suzuki N, Zhou J, Duan DM. Strain capacity of X100 high-strain linepipe for strain-based design application. In: International pipeline conference. 2008. pp. 729–36.
- Kamaya M. Ramberg-Osgood type stress-strain curve estimation using yield and ultimate strengths for failure assessments. *Int J Press Vessels Pip*. 2016;137:1–12. doi:10.1016/j.ijpvp.2015.04.001.
- Limam A, Lee LH, Corona E, Kyriakides S. Inelastic wrinkling and collapse of tubes under combined bending and internal pressure. *Int J Mech Sci*. 2010;52(5):637–47. doi:10.1016/j.ijmecsci.2009.06.008.
- Liu X, Zhang H, Han Y, Xia M, Zheng W. A semi-empirical model for peak strain prediction of buried X80 steel pipelines under compression and bending at strike-slip fault crossings. *J Nat Gas Sci Eng*. 2016;32:465–75. doi:10.1016/j.jngse.2016.04.054.
- Mohareb ME. Deformational behaviour of line pipe. Doctoral dissertation. Edmonton: University of Alberta. 1995.
- Nazemi N. Behavior of X60 line pipe under combined axial and transverse loads with internal pressure. Master thesis. University of Windsor, Windsor, 2009.
- Nobuhisa S, Satoshi I, Katsumi M. Seismic integrity of high-strength pipelines. *JFE Tech Rep*. 2008;17:14–9.
- Ozkan IF, Mohareb M. Moment resistance of steel pipes subjected to combined loads. *Int J Press Vessel Pip*. 2009a;86(4):252–64. doi:10.1016/j.ijpvp.2008.11.013.
- Ozkan IF, Mohareb M. Testing and analysis of steel pipes under bending, tension, and internal pressure. *J Struct Eng*. 2009b;135(2):187–97. doi:10.1061/(ASCE)0733-9445(2009)135:2(187).
- Paquette JA, Kyriakides S. Plastic buckling of tubes under axial compression and internal pressure. *Int J Mech Sci*. 2006;48(8):855–67. doi:10.1016/j.ijmecsci.2006.03.003.
- Ramberg W, Osgood WR. Description of stress-strain curves by three parameters. Technical Report Archive & Image Library. 1943. NACA-TN-902.
- Shantanu J, Prashant A, Arghya D, Sudhir KJ. Analysis of buried pipelines subjected to reverse fault motion. *Soil Dyn Earthq Eng*. 2011;31(7):930–40. doi:10.1016/j.soildyn.2011.02.003.
- Sun YY. Study of perfect pipes on ultimate capacity under complex loads. Master thesis. Dalian: Dalian University of Technology, 2013. (in Chinese).
- Suzuki N, Tajika H, Igi S, Okatsu M, Kondo J, Arakawa T. Local buckling behavior of 48", X80 high-strain line pipes. In: International pipeline conference. 2010.
- Timms CMJ, Degeer DD, Chebaro MR, Tsuru E. Compressive strain limits of large diameter X80 UOE linepipe. In: The 19th international offshore and polar engineering conference. The International Society of Offshore and Polar Engineers. 2009; pp. 181–9.
- Zimmerman T, Timms C, Xie J, Asante J. Buckling resistance of large diameter spiral welded linepipe. In: 2004 international pipeline conference. American Society of Mechanical Engineers, 2004. pp. 365–73. doi:10.1115/IPC2004-0364.